

# Quantum transport length scales in silicon-based semiconducting nanowires: Surface roughness effects

Aurélien Lherbier,<sup>1,2</sup> Martin P. Persson,<sup>2</sup> Yann-Michel Niquet,<sup>2</sup> François Triozon,<sup>3</sup> and Stephan Roche<sup>4</sup><sup>1</sup>Laboratoire des Technologies de la Microélectronique (LTM), UMR 5129 CNRS, CEA, 17 Rue des Martyrs, 38054 Grenoble, France<sup>2</sup>CEA/DSM/DRFMC/SP2M/L\_Sim, 17 rue des Martyrs, 38054 Grenoble Cedex 9, France<sup>3</sup>CEA LETI-MINATEC, 17 rue des Martyrs, 38054 Grenoble Cedex 9, France<sup>4</sup>CEA/DSM/DRFMC/SPSMS/GT, 17 rue des Martyrs, 38054 Grenoble Cedex 9, France

(Received 10 September 2007; published 1 February 2008)

We report on a theoretical study of quantum charge transport in atomistic models of silicon nanowires with surface roughness disorder, using an efficient real-space, order  $N$  Kubo-Greenwood approach and a Landauer-Büttiker Green's function method. Different transport regimes (from quasiballistic to localization) are explored depending on the length of the nanowire and the characteristics of the surface roughness profile. Quantitative estimates of the elastic mean free paths, charge mobilities, and localization lengths are provided as a function of the correlation length of the surface roughness disorder. Moreover, the limitations of the Thouless relation between the mean free path and the localization length are outlined.

DOI: 10.1103/PhysRevB.77.085301

PACS number(s): 73.63.-b, 72.10.-d, 71.23.-k

## I. INTRODUCTION

Semiconducting silicon nanowires (SiNWs) are currently the subject of intense studies due to their prominent role in the downscaling limits of metal-oxide-semiconductor field-effect transistor devices and also because they provide alternative materials to challenge quantum effects in low dimensionality.<sup>1-3</sup> Compared to classical planar technology, nanowires can better accommodate “all-around” gates improving field-effect efficiency and device performances.<sup>4</sup> Vapor-liquid-solid (VLS) growth techniques have recently produced SiNWs with well controlled structural features,<sup>5-7</sup> which open up innovative approaches to the design of silicon-based nanodevices.<sup>8</sup> Demonstrations of  $p$ - $n$  junction diodes,<sup>9</sup> logic gates,<sup>10</sup> field-effect transistors,<sup>11,12</sup> and nanosensors<sup>13,14</sup> have been reported.

However, one key issue in the engineering of performant SiNW-based field-effect transistors (SiNW-FETs) is to ascertain how sensitive the charge mobilities are to structural features such as diameter, growth direction, and disorder. Surface roughness disorder (SRD) is a well-known limiting factor in lithographic SiNW-FETs,<sup>15-17</sup> and its impact on ballistic transport in VLS-grown nanowires is a challenging and important question.<sup>11,12</sup> Besides, SRD effects also raise fundamental questions in the framework of localization theory.<sup>18,19</sup>

Recent *ab initio* studies<sup>20,21</sup> have reported on specific surface effects, such as dopant segregation in small diameter SiNWs. However, most of these studies did not cope with the analysis of the fundamental transport length scales in long disordered nanowires. Several theoretical works have also investigated the role of effective and simplified surface disorder models on the transport properties of nanowire-based materials or devices.<sup>22-27</sup>

In this work, we report on a quantitative analysis of the transport length scales in atomistic models of rough SiNWs. The description of the SiNWs is based on an accurate tight-binding Hamiltonian, previously validated by *ab initio* calculations.<sup>28,29</sup> The quantum transport properties are calcu-

lated with two different approaches. First, the elastic mean free path and the charge mobility are computed with an optimized, real-space, order  $N$  Kubo-Greenwood approach.<sup>30,31</sup> Additionally, the scaling properties of the Landauer-Büttiker conductance are investigated with a standard recursive Green's function method to assess the effects of quantum interferences driving to the localization regime. Both approaches give complementary results and allow us to explore a broad range of conduction mechanisms, from the ballistic to the diffusive and strongly localized regimes. These methods are briefly reviewed in Sec. II, then the results are discussed in Sec. III.

## II. METHODS

### A. Description of the surface roughness profile

The SiNW Hamiltonian is a third nearest neighbor three center orthogonal  $sp^3$  tight-binding model that well describes the electronic structure of ideal (disorder-free) nanowires.<sup>29</sup> The SRD profile is defined as a random fluctuation of the radius of the nanowire around its average value  $R_0$ , characterized by a Lorentzian autocorrelation function.<sup>17,32,33</sup> In cylindrical coordinates,

$$\delta R(z, \theta) = \sum_{(n,k) \neq (0,0)} a_{nk} e^{in\theta} e^{i(2\pi/L)kz}, \quad (1a)$$

$$a_{nk} = \frac{e^{i\varphi_{nk}}}{\left\{ 1 + \left[ \left( \frac{2\pi k}{L} \right)^2 + \left( \frac{n}{R_0} \right)^2 \right] L_r^2 \right\}^{3/4}}. \quad (1b)$$

Here,  $\varphi_{nk} \in [0, 2\pi[$  is a random number,  $L$  is the length of the nanowire, and  $L_r$  is the correlation length of the SRD. The silicon atoms outside the envelope defined by Eq. (1a) are excluded from the nanowire and the dangling bonds are saturated with hydrogen atoms.<sup>34</sup> In the following, we set  $R_0 = 1$  nm and renormalize the  $a_{nk}$  so that  $\langle \delta R^2(z, \theta) \rangle^{1/2} = 1$  Å, leaving  $L_r$  as the only free parameter. The effects of

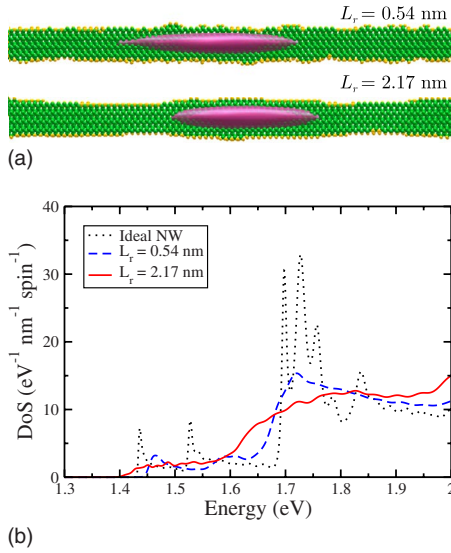


FIG. 1. (Color online) (a) SRD profile and isoprobability surface of the ground-state conduction band wave function of small sections of [110]-oriented SiNWs for two values of  $L_r$ . (b) Corresponding conduction band DoS (dashed and solid lines). The DoS of the ideal nanowire with radius  $R_0=1$  nm is also shown (dotted line).

the SRD on the transport length scales have been computed for [110]-oriented SiNWs with  $L_r$  ranging from 0.54 to 4.34 nm [Fig. 1(a)].

### B. Transport methodologies

In the semiclassical transport theory, the effects of the disorder can be characterized by the scattering rate between the eigenstates of the ideal system.<sup>35</sup> The scattering time  $\tau$ , usually computed with the Fermi's golden rule, can be split into an elastic ( $\tau_e$ ) and an inelastic ( $\tau_i$ ) contribution ( $1/\tau = 1/\tau_e + 1/\tau_i$ ) by virtue of Matthiessen's law. The SRD is expected to dominate backscattering at low temperatures,<sup>15,16</sup> while the inelastic electron-phonon coupling plays a major role at room temperature. In the Kubo-Greenwood approach, the scattering time  $\tau_e(E)$  and the mean free path  $\ell_e(E) = v(E)\tau_e(E)$  are extracted from the saturation of the quantum diffusivity,  $D(E,t) = \Delta Z^2(E,t)/t$ , where  $v(E)$  is the average velocity and  $\Delta Z^2(E,t)$  the quadratic spreading of wave packets with energy  $E$ . Indeed,  $D(E,t)$  behaves as  $v^2(E)t$  for short times  $t$ , then reaches a maximum value  $D_{\max}(E) \approx 2v^2(E)\tau_e(E)$  (diffusive regime), before eventually decreasing due to localization effects (see discussion below).<sup>31</sup>  $\Delta Z^2(E,t)$  is evaluated as

$$\Delta Z^2(E,t) = \frac{\text{Tr}\{[\hat{Z}(t) - \hat{Z}(0)]^2 \delta(E - \hat{H})\}}{\text{Tr}\{\delta(E - \hat{H})\}}, \quad (2)$$

where  $\hat{Z}(t)$  is the position operator in the Heisenberg representation,  $\delta(E - \hat{H})$  is the spectral measure of the SiNW Hamiltonian, and Tr is the trace over the  $sp^3$  basis set. Periodic boundary conditions are applied along the nanowire, the convergence being achieved for supercell lengths  $L$

$\approx 500$  nm. The real-space, order  $N$  methodology of Ref. 31 has been adapted to this multiorbital per site problem. In particular, we have used the kernel polynomial method<sup>36</sup> to compute the spectral quantities from the Lanczos recursion coefficients.<sup>37</sup> This provides a more accurate description of the band edges than the usual continued fraction expansion.<sup>26,31,38</sup>

In the absence of inelastic scattering, quantum interferences build up beyond the diffusive regime, which leads to the localization of all wave functions in the zero-temperature limit.<sup>18,39,40</sup> The conductance of long nanowires in the strong localization regime can therefore be characterized by the localization length  $\xi(E)$

$$\langle \ln g(E,L) \rangle \sim -2L/\xi(E), \quad (3)$$

where  $g(E,L) = G(E,L)/G_0$  is the normalized conductance of wires with length  $L$  ( $G_0 = 2e^2/h$  being the quantum of conductance) and  $\langle \dots \rangle$  is a statistical average over different realizations of the disorder.  $g(E,L)$  can be conveniently computed in the Landauer-Büttiker Green's function framework.<sup>33</sup> This method is indeed well suited to the description of finite-size nanowires connected to drain and source electrodes. The latter are modeled as ideal, semi-infinite nanowires with radius  $R = R_0 + 0.2$  nm. The transmission through the device is computed from the self-energies of the contacts and Green's function of the nanowire using a standard decimation technique.<sup>26,41</sup>

## III. RESULTS AND DISCUSSION

### A. Electronic properties

Let us first discuss the electronic structure of the SiNWs. The conduction band density of states (DoS)  $\rho(E)$  for the ideal and for two disordered SiNWs are shown in Fig. 1(b). In the ideal SiNW, the first two Van Hove singularities (VHs's) arise from the [001] bulk conduction band minima<sup>29</sup> and are split by the intervalley couplings, while the others (above 1.7 eV) arise from both [001] and {[100], [010]} minima. The DoS is markedly affected by the SRD. At  $L_r = 0.54$  nm, the lowest-lying VHs's are shifted to higher energies, as a result of the increase of the average lateral confinement within the SiNW. However, with increasing  $L_r$ , the conduction band edge moves to lower energy, while the DoS is steadily degraded, hardly showing any fine structure for  $L_r \geq 2.17$  nm. The lowest-lying conduction band states are indeed trapped deeper in energy in the largest sections of the nanowire [see Fig. 1(a)]. The extent of the electron wave functions will ultimately determine the transport regime.<sup>42</sup>

### B. Elastic mean free paths and charge mobilities

The mean free path of the electrons and holes is plotted as a function of their energy in Fig. 2 for the same two  $L_r$  as in Fig. 1. The main features of the underlying band structure still show up at  $L_r = 0.54$  nm. Indeed, the electron mean free path reaches its maximum ( $\ell_e \approx 70$  nm) between the first two VHs's (single subband transport), which shows a dip at the edge of the second subband, then further decreases above  $E \approx 1.7$  eV due to the enhancement of interband scattering.

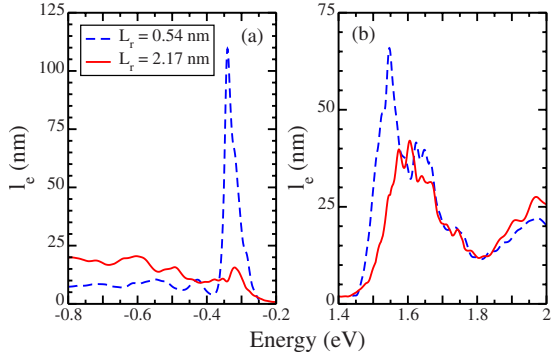


FIG. 2. (Color online) Mean free path of the (a) holes and (b) electrons as a function of energy for  $L_r=0.54$  nm and  $L_r=2.17$  nm.

The hole mean free path also exhibits a very sharp peak ( $\ell_e \simeq 110$  nm) in the first (mostly light-hole) subband, but it becomes very short in the dense, lower-lying subbands. However, at  $L_r=2.17$  nm, the fine structure of  $\ell_e$  cannot be so easily related to the band structure of the ideal nanowire. The mean free path is almost reduced by half in the first electron “subband,” while the peak on the valence band side is nearly five times smaller and is superseded by a broad feature at lower energies.

The charge carrier mobility  $\mu$  is another key quantity for assessing device performances. In absence of strong inelastic scattering processes, it can be related to the Kubo conductivity,

$$\begin{aligned} \sigma(E_F) &= n(E_F)\mu(E_F)e \\ &= -\frac{e^2}{2} \int dE \rho(E) D_{\max}(E) \frac{\partial f_{FD}(E-E_F)}{\partial E}, \end{aligned} \quad (4)$$

where  $n(E_F) = \int dE \rho(E) f_{FD}(E-E_F)$  is the charge density (per unit of length) at a given Fermi energy  $E_F$ ,  $e$  is the elementary charge, and  $f_{FD}(E)$  is the Fermi-Dirac distribution function.<sup>31,33</sup> The mobility  $\mu(E_F)$  is plotted as a function of  $E_F$  in Fig. 3 for  $L_r=0.54$  nm and  $L_r=2.17$  nm, both at  $T \rightarrow 0$  K and at room temperature ( $T=300$  K). The low temperature mobility follows the same trends as  $\ell_e$ . In particular,

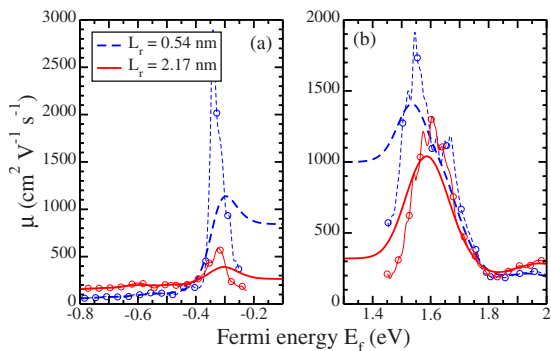


FIG. 3. (Color online) Mobility of the (a) holes and (b) electrons as a function of the Fermi energy  $E_F$  for  $L_r=0.54$  nm and  $L_r=2.17$  nm. The mobility is plotted both at  $T \rightarrow 0$  K (symbols) and  $T=300$  K (thick lines).

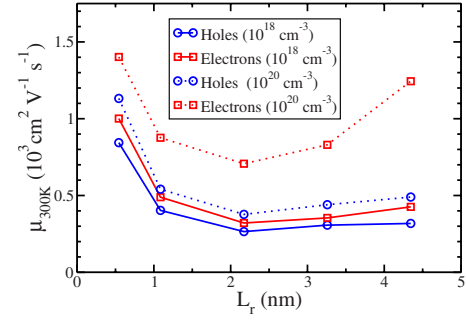


FIG. 4. (Color online) Room-temperature mobility of the electrons and holes as a function of  $L_r$  for two electron and/or hole densities  $n=10^{18}$   $\text{cm}^{-3}$  and  $n=10^{20}$   $\text{cm}^{-3}$ .

$\mu(E_F)$  is much lower around the conduction and valence band edges, where the wave functions tend to localize in the largest sections of the nanowires. The room-temperature mobility  $\mu_{300\text{K}}$ , which averages over the Fermi-Dirac distribution, is more significant in this range (but might be further limited by phonon scattering). As a matter of fact,  $\mu_{300\text{K}}$  is almost constant for Fermi energies corresponding to electron and hole densities up to  $n \simeq 10^{19}$   $\text{cm}^{-3}$ . It peaks around  $n = 10^{20}$   $\text{cm}^{-3}$  then rapidly decreases. The values of  $\mu_{300\text{K}}$  at  $n=10^{18}$   $\text{cm}^{-3}$  and  $n=10^{20}$   $\text{cm}^{-3}$  are reported as a function of  $L_r$  in Fig. 4. They are comparable for electrons and holes in the low-density limit, and are ranging from a few hundreds to  $\sim 1000$   $\text{cm}^2 \text{V}^{-1} \text{s}^{-1}$ , in fair agreement with the experimental estimates for the most performant undoped silicon nanowires.<sup>11</sup> The mobility moreover shows a minimum as a function of  $L_r$ . This suggests that the electrons and holes are less sensitive to short length scale fluctuations of the SRD profile.<sup>43</sup> They are much more efficiently scattered at intermediate values of  $L_r$ , while the mobility slowly increases at large  $L_r$  as the surface of the nanowires becomes locally smooth again. The mobility is still, however, quite smaller around the conduction and valence band edges (i.e., at low densities), as evidenced in Fig. 4.

### C. Conductance, quantum interference effects, and localization regime

In the absence of disorder, the transport through the SiNWs is ballistic so that the Landauer-Büttiker conductance  $G(E) = N_{\perp} G_0$  is quantized and independent of the wire length  $L$ ,  $N_{\perp}$  being the number of conducting channels at energy  $E$ . This is illustrated in Fig. 5(d).<sup>44</sup> Conductance quantization has actually been observed in narrow constrictions (quantum point contacts) made on silicon<sup>45</sup> and silicon wires.<sup>11,46</sup> The conductance is expected to scale as  $\ell_e/L$ , in short, weakly disordered nanowires;<sup>40</sup> however, most of the results available on longer and wider, lithographically defined SiNWs evidence strong disorder effects (due to wire width fluctuations or charged impurities) such as quantum interferences, localization,<sup>47</sup> and charging phenomena.<sup>48,49</sup>

In this work, we neglect the effects of inelastic scattering and focus on the transition from weak to strong localization. The localization length  $\xi(E)$ , computed from the scaling

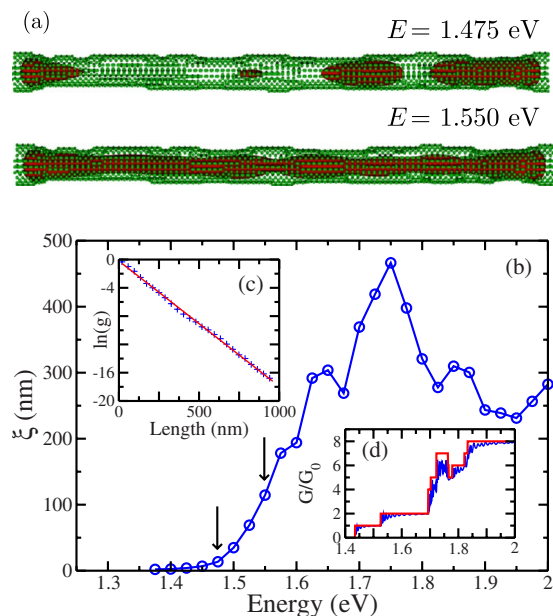


FIG. 5. (Color online) (a) Local density of states in a short nanowire with length  $L \approx 30$  nm at energies  $E = 1.475$  eV and  $E = 1.55$  eV [arrows in (b)]. (b) Localization length  $\xi$  as a function of energy ( $L_r = 2.17$  nm). (c) Linear fit (red solid line) to  $\langle \ln g \rangle / L$  (blue crosses) at  $E = 1.55$  eV. (d) Landauer-Büttiker conductance of an ideal nanowire ( $R_0 = 1$  nm) (Ref. 44) along with the number of conducting channels (staircase line).

analysis of the Landauer-Büttiker conductance (see Sec. II B), is plotted as a function of the conduction band energy in Fig. 5(b) ( $L_r = 2.17$  nm). The logarithm of  $g$  was averaged (for each  $L$ ) over 150 random SRD profiles [Fig. 5(c)].  $\xi$  ranges from a few nanometers close to the gap up to  $\approx 500$  nm at higher energies. The electrons indeed tend to localize in the largest sections of the nanowires near the conduction band edge [see Fig. 1(a)]. As another illustration, the local density of states is shown at two conduction band energies in Fig. 5(a) for a short nanowire with length  $L \approx 30$  nm. The corresponding localization lengths are  $\xi(1.475 \text{ eV}) = 13.5$  nm and  $\xi(1.55 \text{ eV}) = 114.5$  nm.

In weakly disordered quasi-one-dimensional (quasi-1D) systems, the fundamental length scales  $\xi$  and  $\ell_e$  are expected to fulfill the relation  $\xi \sim 2(N_{\perp} + 1)\ell_e$ .<sup>39,50</sup> This relation was first established by Thouless<sup>39</sup> for strictly one-dimensional systems then further generalized using random matrix theory to weakly disordered quasi-1D systems with a large number of conducting channels.<sup>40</sup> Recently, it has been challenged numerically in models of chemically doped, disordered carbon nanotubes.<sup>51</sup> The  $\xi/(2\ell_e)$  ratio in SiNWs is compared to  $N_{\perp} + 1$  (deduced from the band structure of the ideal nano-

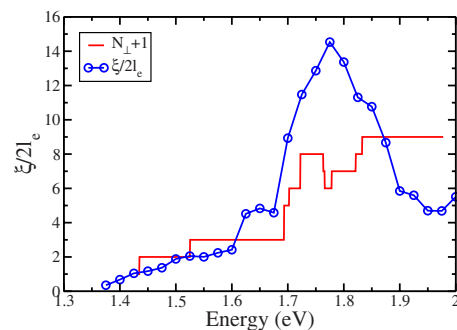


FIG. 6. (Color online)  $\xi/(2\ell_e)$  and  $N_{\perp} + 1$  as a function of energy.

wire) in Fig. 6. As evidenced by our calculations,  $\xi/(2\ell_e)$  roughly scales as  $N_{\perp} + 1$  close to the conduction band edge, but not at higher energies. These discrepancies likely arise because the surface roughness induces large changes in the electronic structure of such thin Si nanowires (as shown in Fig. 1), which hinder the identification of a well-defined channel structure. Similar discrepancies were also recently reported in simplified models of disordered quantum wires, but in the presence of a magnetic field.<sup>19</sup>

#### IV. CONCLUSION

In conclusion, some key transport length scales have been investigated in disordered semiconductor nanowires using an optimized real-space, order  $N$  Kubo-Greenwood method combined with a recursive Green's function based Landauer-Büttiker approach. The effectiveness of an atomistic surface roughness profile in limiting transport has been demonstrated, and the trends in the energy-dependent electron and hole mobilities, mean free paths, and localization lengths have been discussed at a quantitative level. The limitations of the Thouless relation in such complex disordered systems have also been pointed out. Other studies focusing on the role of nanowire orientation, diameter, and on other kind of disorders such as dopants,<sup>29,52</sup> surface defects, or oxide traps deserve further consideration. Moreover, the impact of disorder on SiNW-based field-effect devices should also be investigated,<sup>53</sup> beyond its intrinsic effects on the transport length scales.

#### ACKNOWLEDGMENTS

This work was supported by the French ‘‘Action Concert e Initiative’’ (ACI) ‘‘Transnanofils’’ and by the EU under Project No. 015783 NODE. The calculations were performed at the CEA/CCRT supercomputing center, and the ‘‘CEA ChimTronique programme’’ is acknowledged for technical support.

- <sup>1</sup>A. E. Hansen, M. T. Björk, C. Fasth, C. Thelander, and L. Samuelson, *Phys. Rev. B* **71**, 205328 (2005).
- <sup>2</sup>Z. Zhong, Y. Fang, W. Lu, and C. M. Lieber, *Nano Lett.* **5**, 1143 (2005).
- <sup>3</sup>Y.-J. Doh, J. A. van Dam, A. L. Roest, E. P. A. M. Bakkers, L. P. Kouwenhoven, and S. De Franceschi, *Science* **309**, 272 (2005).
- <sup>4</sup>J. P. Colinge, *Solid-State Electron.* **48**, 897 (2004).
- <sup>5</sup>D. D. Ma, C. S. Lee, F. C. K. Au, S. Y. Tong, and S. T. Lee, *Science* **299**, 1874 (2003).
- <sup>6</sup>Y. Wu, Y. Cui, L. Huynh, C. J. Barrelet, D. C. Bell, and C. M. Lieber, *Nano Lett.* **4**, 433 (2004).
- <sup>7</sup>K. A. Dick, K. Deppert, T. Mårtensson, B. Mandl, L. Samuelson, and W. Seifert, *Nano Lett.* **5**, 761 (2005).
- <sup>8</sup>M. T. Björk, B. J. Ohlsson, T. Sass, A. I. Persson, C. Thelander, M. H. Magnusson, K. Deppert, L. R. Wallenberg, and L. Samuelson, *Nano Lett.* **2**, 87 (2002).
- <sup>9</sup>Y. Cui and C. M. Lieber, *Science* **291**, 851 (2001).
- <sup>10</sup>Y. Huang, X. Duan, Y. Cui, L. J. Lauhon, K.-H. Kim, and C. M. Lieber, *Science* **294**, 1313 (2001).
- <sup>11</sup>Y. Cui, Z. Zhong, D. Wang, W. U. Wang, and C. M. Lieber, *Nano Lett.* **3**, 149 (2003).
- <sup>12</sup>J. Xiang, W. Lu, Y. Hu, Y. Wu, H. Yan, and C. M. Lieber, *Nature (London)* **441**, 489 (2006).
- <sup>13</sup>Y. Cui, Q. Wei, H. Park, and C. M. Lieber, *Science* **293**, 1289 (2001).
- <sup>14</sup>F. Patolsky, G. Zheng, O. Hayden, M. Lakadamyali, X. Zhuang, and C. M. Lieber, *Proc. Natl. Acad. Sci. U.S.A.* **101**, 14017 (2004).
- <sup>15</sup>R. van Langevelde and F. M. Klaassen, *IEEE Trans. Electron Devices* **44**, 2044 (1997).
- <sup>16</sup>A. K. Sharma, S. H. Zaidi, S. Lucero, S. R. J. Brueck, and N. E. Islam, *IEE Proc.: Circuits Devices Syst.* **151**, 422 (2004).
- <sup>17</sup>J. Wang, E. Polizzi, A. Ghosh, S. Datta, and M. Lundstrom, *Appl. Phys. Lett.* **87**, 043101 (2005).
- <sup>18</sup>L. S. Froufe-Pérez, P. García-Mochales, P. A. Serena, P. A. Mello, and J. J. Sáenz, *Phys. Rev. Lett.* **89**, 246403 (2002); *Microelectron. J.* **36**, 893 (2005).
- <sup>19</sup>J. Feist, A. Bäcker, R. Ketzmerick, S. Rotter, B. Huckestein, and J. Burgdörfer, *Phys. Rev. Lett.* **97**, 116804 (2006).
- <sup>20</sup>R. Rurali and N. Lorente, *Phys. Rev. Lett.* **94**, 026805 (2005); *Nanotechnology* **16**, S250 (2005).
- <sup>21</sup>M. V. Fernandez-Serra, Ch. Adessi, and X. Blase, *Phys. Rev. Lett.* **96**, 166805 (2006); *Nano Lett.* **6**, 2674 (2006).
- <sup>22</sup>D. Csontos and H. Q. Xu, *Appl. Phys. Lett.* **77**, 2364 (2000).
- <sup>23</sup>J. Zhong and G. M. Stocks, *Nano Lett.* **6**, 128 (2006).
- <sup>24</sup>Y. Takagaki and D. K. Ferry, *J. Phys.: Condens. Matter* **4**, 10421 (1992).
- <sup>25</sup>K. Nikolić and A. MacKinnon, *Phys. Rev. B* **50**, 11008 (1994).
- <sup>26</sup>T. Markussen, R. Rurali, M. Brandbyge, and A.-P. Jauho, *Phys. Rev. B* **74**, 245313 (2006).
- <sup>27</sup>A. Svizhenko, P. W. Leu, and K. Cho, *Phys. Rev. B* **75**, 125417 (2007).
- <sup>28</sup>Y. M. Niquet, C. Delerue, G. Allan, and M. Lannoo, *Phys. Rev. B* **62**, 5109 (2000).
- <sup>29</sup>Y. M. Niquet, A. Lherbier, N. H. Quang, M. V. Fernandez-Serra, X. Blase, and C. Delerue, *Phys. Rev. B* **73**, 165319 (2006).
- <sup>30</sup>R. Kubo, *Rep. Prog. Phys.* **29**, 255 (1966).
- <sup>31</sup>S. Roche and D. Mayou, *Phys. Rev. Lett.* **79**, 2518 (1997); S. Roche, *Phys. Rev. B* **59**, 2284 (1999); S. Roche and R. Saito, *Phys. Rev. Lett.* **87**, 246803 (2001); F. Triozon, S. Roche, A. Rubio, and D. Mayou, *Phys. Rev. B* **69**, 121410(R) (2004); S. Latil, S. Roche, D. Mayou, and J.-C. Charlier, *Phys. Rev. Lett.* **92**, 256805 (2004).
- <sup>32</sup>S. M. Goodnick, D. K. Ferry, C. W. Wilmsen, Z. Liliental, D. Fathy, and O. L. Krivanek, *Phys. Rev. B* **32**, 8171 (1985).
- <sup>33</sup>D. K. Ferry and S. M. Goodnick, *Transport in Nanostructures* (Cambridge University Press, Cambridge, 1997), and references therein.
- <sup>34</sup>All silicon atoms that end up with three hydrogen atoms as first nearest neighbors are also removed from the nanowire and replaced with a single hydrogen atom.
- <sup>35</sup>N. F. Mott and E. A. Davis, *Electronic Processes in Non Crystalline Materials*, 1st ed. (Clarendon, Oxford, 1971), p. 20.
- <sup>36</sup>A. Weiße, G. Wellein, A. Alvermann, and H. Fehske, *Rev. Mod. Phys.* **78**, 275 (2006).
- <sup>37</sup>G. Allan, *J. Phys. C* **17**, 3945 (1984).
- <sup>38</sup>The Kubo data were averaged over five to ten realizations of the SRD, the trace being computed with eight random-phase states.
- <sup>39</sup>D. J. Thouless, *Phys. Rev. Lett.* **39**, 1167 (1977).
- <sup>40</sup>C. W. J. Beenakker, *Rev. Mod. Phys.* **69**, 731 (1997).
- <sup>41</sup>G. Grosso, S. Moroni, and G. P. Parravicini, *Phys. Rev. B* **40**, 12328 (1989); F. Triozon, Ph. Lambin, and S. Roche, *Nanotechnology* **16**, 230 (2005).
- <sup>42</sup>J. Dong and D. A. Drabold, *Phys. Rev. Lett.* **80**, 1928 (1998).
- <sup>43</sup>N. Trivedi and N. W. Ashcroft, *Phys. Rev. B* **38**, 12298 (1988).
- <sup>44</sup>In the Landauer-Büttiker approach, the ideal and disordered SiNWs are connected to slightly larger SiNW electrodes, which gives rise to the Fabry-Perot-like oscillations visible in the inset of Fig. 5(d).
- <sup>45</sup>D. Többen, D. A. Wharam, G. Abstreiter, J. P. Kotthaus, and F. Schäffler, *Semicond. Sci. Technol.* **10**, 711 (1995).
- <sup>46</sup>Y. Takahashi, A. Fujiwara, and K. Murase, *Semicond. Sci. Technol.* **13**, 1047 (1998).
- <sup>47</sup>A. T. Tilke, F. C. Simmel, H. Lorenz, R. H. Blick, and J. P. Kotthaus, *Phys. Rev. B* **68**, 075311 (2003).
- <sup>48</sup>L. Zhuang, L. Guo, and S. Y. Chou, *Appl. Phys. Lett.* **72**, 1205 (1998).
- <sup>49</sup>M. Sanquer, M. Specht, L. Ghenim, S. Deleonibus, and G. Guegan, *Phys. Rev. B* **61**, 7249 (2000).
- <sup>50</sup>Our mean free path  $\ell_e = v\tau_e$ , consistent with kinetic theory, is half the mean free path defined, e.g., in Ref. 40—hence, the additional factor of 2 in Thouless relation.
- <sup>51</sup>R. Avriller, S. Latil, F. Triozon, X. Blase, and S. Roche, *Phys. Rev. B* **74**, 121406(R) (2006).
- <sup>52</sup>T. Markussen, R. Rurali, A.-P. Jauho, and M. Brandbyge, *Phys. Rev. Lett.* **99**, 076803 (2007).
- <sup>53</sup>J. Wang, A. Rahman, A. Ghosh, G. Klimeck, and M. Lundstrom, *IEEE Trans. Electron Devices* **52**, 1589 (2005); Y. Zheng, C. Rivas, R. Lake, K. Alam, T. B. Boykin, and G. Klimeck, *ibid.* **52**, 1097 (2005); A. Martinez, M. Bescond, J. R. Barker, A. Svizhenko, M. P. Anantram, C. Millar, and A. Asenov, *ibid.* **54**, 2213 (2007).